

Conformational Analysis of Guaianolide-Type Sesquiterpene Lactones by Low-Temperature NMR Spectroscopy and Semiempirical Calculations

Slobodan Milosavljević,¹ Ivan Juranić,¹ Vanja Bulatović,² Slobodan Macura,³ Nenad Juranić,³ Hans-Heinrich Limbach,⁴ Klaus Weisz,⁴ Vlatka Vajs,⁵ and Nina Todorović^{5,6}

Received June 26, 2003; revised September 11, 2003; accepted September 29, 2003

Conformational analysis of 9 α -acetoxycumambrine A **1** and 8-*O*-isobutiryl-9 α -acetoxycumambrine B **2** was carried out by low-temperature NMR studies. Results suggested that lactones **1** and **2** are mixtures of two distinctive conformers, I and II. Based on low-temperature ¹H NMR spectra, in four solvents, the thermodynamic parameters of I \rightleftharpoons II exchange process were assessed. Energy of activation of I \rightarrow II reaction was obtained by dynamic NMR simulations for both compounds. Results revealed that conformational exchange of lactones **1** and **2** occurs due to "chair \rightleftharpoons twisted chair" interconversion of a heptane ring. The same PM3 semiempirical method was applied for geometry optimization of lactones **1** and **2**, as well as of 9 α -hydroxycumambrine A **3**, 9 α -acetoxycumambrine B **4**, and cumambrine B **5**.

KEY WORDS: Guaianolides; cumambrine; conformations; low-temperature NMR; dynamic NMR; PM3 semiempirical calculations.

INTRODUCTION

Chemotaxonomic importance of the natural sesquiterpene lactones, as well as their prominent and diverse physiological activity, are the major reasons for continuous interest regarding these compounds. It was pointed out that their activity is most likely associated with the α , β -methylene γ -lactone part of a molecule. Nevertheless, in addition to structural demands, it is well known that geometry of the entire molecule is important for the expression of biological activity.

Accordingly, elucidation of conformational properties of these compounds could be interesting. During the last few decades, an appreciable number of sesquiterpene lactones has been isolated from the plant sources and guaianolides represent one of the most abundant group. However, conformational analysis of guaianolides received relatively little attention [1] and, having in mind numerous conformational possibilities of a heptane ring, papers about conformational exchange phenomena of guaianolides are surprisingly rare [2].

Recently, we have reported isolation and structure determination of conformationally flexible guaianolides **1** and **2** (Fig. 1) [2a, b]. Well-known cumambrine B **5** was isolated on the same occasion [2b]. Also, as a part of our previous investigations, the inseparable structural isomers **3** and **4** (Fig. 1) were isolated as a mixture (3/4 = 15/85) and their structures were fully determined by NMR spectra of the mixture [2c]. These NMR spectra unambiguously showed that lactone **4** is in conformational equilibrium, contrary to its structural isomer **3**.

¹Faculty of Chemistry, University of Belgrade, 11000 Belgrade, Serbia and Montenegro.

²Institute for Medicinal Plant Research "Dr. Josif Pančić," 11000 Belgrade, Serbia and Montenegro.

³Department of Biochemistry and Molecular Biology, Mayo Foundation, Rochester, Minnesota 55905.

⁴Institut für Chemie, Freie Universität Berlin, Berlin, Germany.

⁵Institute for Chemistry, Technology and Metallurgy, Njegoševa 12, 11000 Belgrade, Serbia and Montenegro.

⁶To whom correspondence should be addressed; e-mail: ninat@chem.bg.ac.yu

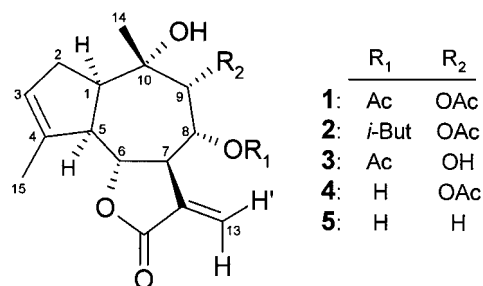


Fig. 1. Guaianolides 1–5.

Herein we present an investigation of the conformational equilibrium of lactones **1** and **2** by low-temperature NMR experiments and evaluation of the conformations of all five guaianolides **1–5** (Fig. 1) by the PM3 semiempirical method.

EXPERIMENTAL

Guaianolides **1–5** originate from plant species *Anthemis carpatica* and their isolation and structure determination were reported elsewhere [2a–c].

NMR STUDIES

The NMR spectra were measured with Bruker DRX300 (operating at 300.13 MHz for ¹H) and Bruker DRX500 (operating at 500.13 MHz for ¹H) spectrometers, in deuterated solvents. Coupling constants (*J*) are given in Hz and chemical shifts (δ) are reported relative to TMS as internal standard. The 5-mm double resonance probeheads ¹H/¹³C were used at both spectrometers and were kept at room temperature by an external thermostat, so only the sample tube was cooled down to the required temperatures. The temperatures were adjusted by Eurotherm Variable Temperature Unit using the external devices, “thermocouple K” and “Pt-100-thermo,” for Bruker DRX300 and Bruker DRX500, respectively. All temperatures were measured to an accuracy of $\pm 1^\circ\text{C}$.

The conformational exchange I \rightleftharpoons II of compounds **1** and **2** was investigated by two sets of ¹H NMR experiments: (1) All 1D ¹H NMR measurements for elucidating thermodynamic parameters of the exchange process were performed with Bruker DRX300 spectrometer, in methylene chloride-*d*₂, methanol-*d*₄, acetone-*d*₆, and toluene-*d*₈, at six temperatures in a range of ≈ 180 to 240 K. The temperature scale was calibrated with methanol by standard procedure [3]. The line shapes of spectra below

250 K revealed a slow exchange regime; hence, those signals that are not affected by impurities, or overlapped with other signals, could be reliably integrated. The equilibrium constants $K_{\text{I-II}} = [\text{II}]/[\text{I}]$ were obtained as the ratio of the integrals of relevant, separated ¹H signals of conformers I and II. The signals selected for integration were: 13-H, 6-H, and 7-H in CD₂Cl₂ and CD₃OD, 13-H and 15-H in (CD₃)₂CO, and 13-H and 13'-H in C₇D₈. (2) The series of 1D ¹H NMR spectra for band-shape analysis were recorded with Bruker AMX500, in CD₂Cl₂, over a temperature range of 233 to 313 K. All acquisition and processing parameters were exactly the same for compounds **1** and **2**, except a number of scans (ns); calculated concentrations were 2 mg cm⁻³ (ns = 256) and 5 mg·cm⁻³ (ns = 64), for compounds **1** and **2**, respectively. Previous ¹H NMR experiments revealed that there was no concentration dependence associated with chemical shifts, line widths, or signals intensities. Dynamic NMR simulations were achieved using in-house⁷ developed programs based on the quantum-mechanical matrix formalism of Binsch [4]. The spectrum at 233 K was treated as having a zero interconversion rate for both compounds, **1** and **2**, and for both interconverting species, I and II.

Theoretical Calculations

The energy minimization of lactones **1–5** was performed by semiempirical quantum mechanical PM3 method comprised in HyperChem 4.0 program package, applying Polak–Ribiere minimization algorithm. Starting structures were created with HyperChem and initially minimized to RMS gradient less than 0.05 kcal·Å⁻¹·mol⁻¹. The conformational search was performed applying a direct search method and standard settings. All rotatable cyclic bonds were included as variable torsions and allowed to change simultaneously. Acyl side chains were included in the conformational search. The resulting structures were energy minimized to a RMS gradient as above.

RESULTS AND DISCUSSIONS

Conformational Analysis of 9 α -Acetoxycumambrine A (**1**) and 8-*O*-Isobutiryl-9 α -acetoxycumambrine B (**2**)

Thermodynamic Parameters of the Exchange Process

The NMR results show a high degree of analogy in conformational behavior of compounds **1** and **2**. Broad

⁷AG Limbach, Institut für Chemie, Freie Universität Berlin.

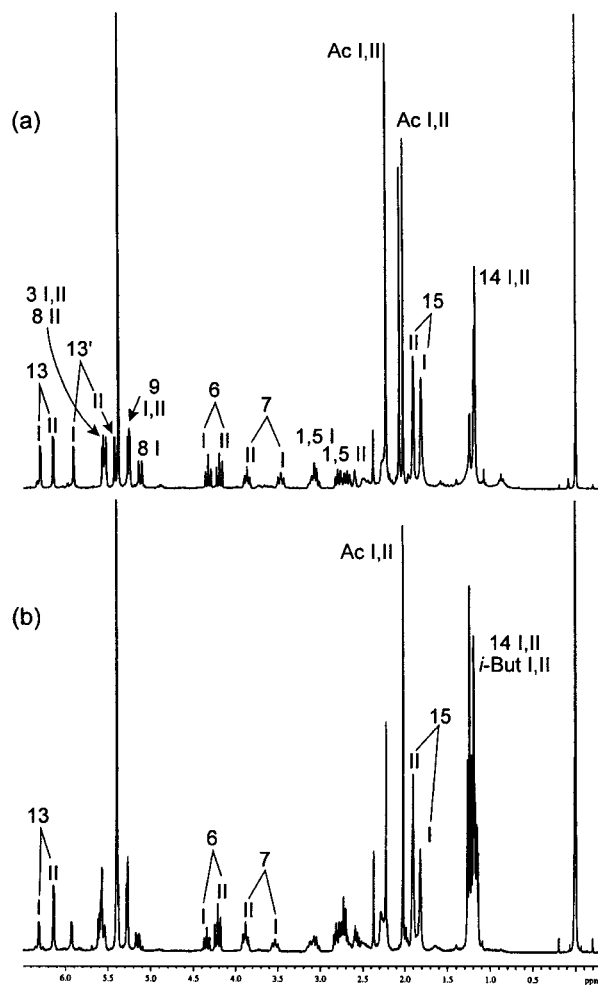


Fig. 2. ^1H NMR spectra (CD_2Cl_2) of: (a) compound **1**, $T = 214$ K, $I/II = 1/1.2$; (b) compound **2**, $T = 217$ K, $I/II = 1/2$.

lines in their room-temperature NMR spectra are typical for the conformational exchange of a medium rate on NMR time scale. For both lactones, coalescence point was at $T_c = 278$ K and below 253 K most of ^1H and ^{13}C NMR signals split into pairs of sharp, well-resolved

resonances, thus indicating presence of two conformers, I and II (Fig. 2). Within each pair in PS-NOESY, the ^1H signals were connected by positive cross peaks, characteristic for slow-exchanging conformers [2(a,b)]. Apart from the consistent difference in chemical shifts of the corresponding NMR signals, the conformers exhibited different vicinal couplings of 8-H to 7-H and 9-H: $J_{7,8} \approx 11$, $J_{8,9} \approx 2.5$ Hz and $J_{7,8} \approx 9$, $J_{8,9} \approx 5$ Hz, for conformers I and II, respectively.

We have recorded ^1H NMR spectra of lactones **1** and **2** in four solvents, in temperature range of ≈ 180 to 240 K and conformer distributions are estimated on the integral values of the suitable ^1H NMR signals (Table I).

Variable-temperature ^1H NMR measurements revealed the increasing population of conformer II at the expense of I, with temperature increases (Table I). Apparently, conformer distribution virtually depends on the dielectric constant of the solvent. In polar solvents [CD_3OD , $(\text{CD}_3)_2\text{CO}$], conformer I predominates over the entire temperature range, for **1** and **2**. In nonpolar solvents (CD_2Cl_2 , C_7D_8) conformer distribution is much more dependent on temperature than in polar ones (Table I). From the ratios of the integrals of the appropriate ^1H NMR signals (given in parenthesis), at six temperatures (calibrated by methanol), in four solvents, equilibrium constants $K_{I-II} = [II]/[I]$ for the exchange reaction $I \rightleftharpoons II$ were obtained (Tables II and III).

The thermodynamic parameters ΔH° and ΔS° of the exchange process, obtained by linear regression analysis from Eq. (1), indicate that we are dealing with mixture of the conformers of comparable stabilities (enthalpies), while free-energy change of the $I \rightleftharpoons II$ reaction includes considerable contribution of the free entropy difference (Tables IV and V).

$$\ln K = -\Delta G^\circ/RT = -\Delta H^\circ/RT + \Delta S^\circ/R \quad (1)$$

Presumably, the main term in, relatively large, ΔS° of the exchange process belongs to the entropy of mixing, favoring conformation II at higher temperatures, particularly in nonpolar solvents.

Table I. Conformer Populations (%) for Lactones **1** and **2** According to ^1H NMR Spectra in Different Solvents at the Ends of Temperature Range (Approximate Temperature Values)

Compound	Conformer	CD_2Cl_2		CD_3OD		$(\text{CD}_3)_2\text{CO}$		C_7D_8	
		180 K	240 K	180 K	240 K	180 K	240 K	180 K	240 K
1	I	56	47.6	87.8	80	80.7	75.2	80	55.9
	II	44	52.4	12.2	20	19.3	24.8	20	44.1
2	I	35	31.5	87.8	80.3	81.1	73.4	61.9	40.6
	II	65	68.5	12.2	19.7	18.9	26.6	38.1	59.4

Table II. Equilibrium Constants K_{I-II} for Lactone **1**: CD₂Cl₂, CD₃OD, (CD₃)₂CO, and C₇D₈

T_{calib} (K)	K_{I-II}			T_{calib} (K)	K_{I-II}		
	(13-H)	(6-H)	(7-H)		(13-H)	(6-H)	(7-H)
	CD ₂ Cl ₂				CD ₃ OD		
180.17	0.803	0.831	0.707	180.17	0.145	0.132	^a
192.65	0.886	0.950	0.774	192.65	0.147	0.148	^a
203.57	0.987	1.040	0.899	204.93	0.173	0.175	0.189
217.02	1.070	1.111	0.980	218.35	0.192	0.208	0.215
228.91	1.136	1.155	1.009	228.91	0.22	0.242	0.234
243.19	1.114	1.181	1.031	240.61	0.252	0.250	0.240
T_{calib} (K)	K_{I-II}		T_{calib} (K)	K_{I-II}			
	(13-H)	(15-H)		(13-H)	(13'-H)		
	(CD ₃) ₂ CO			C ₇ D ₈			
178.77	0.184	0.247	180.17	0.252	^a		
191.27	0.232	0.255	192.65	0.319	^a		
203.57	0.241	0.278	203.57	0.503	0.47		
215.68	0.252	0.325	215.68	0.625	0.59		
227.6	0.265	0.350	227.6	0.727	0.657		
241.90	0.287	0.339	243.19	0.827	0.763		

^aThe signal is overlapped.**Table III.** Equilibrium Constants K_{I-II} for Lactone **2**: CD₂Cl₂, CD₃OD, (CD₃)₂CO, and C₇D₈

T_{calib} (K)	K_{I-II}			T_{calib} (K)	K_{I-II}		
	(13-H)	(6-H)	(7-H)		(13-H)	(6-H)	(7-H)
	CD ₂ Cl ₂				CD ₃ OD		
181.57	1.937	1.861	1.748	180.17	0.128	0.151	0.142
192.65	2.190	2.128	1.954	192.65	0.149	0.131	0.123
203.57	2.139	2.065	1.918	204.93	0.183	0.171	0.149
214.39	2.220	2.122	1.959	217.02	0.195	0.204	0.167
227.6	2.150	2.136	1.958	228.91	0.234	0.246	0.208
244.47	2.397	2.171	2.00	241.9	0.259	0.257	0.227
T_{calib} (K)	K_{I-II}		T_{calib} (K)	K_{I-II}			
	(13-H)	(15-H)		(13-H)	(13'-H)		
	(CD ₃) ₂ CO			C ₇ D ₈			
180.17	0.208	0.237	180.17	0.616	^a		
191.27	0.240	0.256	192.65	0.803	^a		
203.57	0.285	0.308	204.93	1.002	1.027		
217.02	0.341	0.336	215.68	1.128	1.161		
228.91	0.375	0.352	228.91	1.34	1.374		
241.90	0.355	0.394	241.90	1.426	1.505		

^aThe signal is overlapped.**Table IV.** Thermodynamic Parameters of I \rightleftharpoons II Process for Lactones **1** and **2** Obtained from Linear Plot of Eq. (1)

Compd	CD ₂ Cl ₂		CD ₃ OD		(CD ₃) ₂ CO		C ₇ D ₈	
	$\Delta H^{\circ a}$	$\Delta S^{\circ b}$	ΔH°	ΔS°	ΔH°	ΔS°	ΔH°	ΔS°
1	0.52 ± 0.07	2.41 ± 0.35	0.9 ± 0.05	0.97 ± 0.26	0.53 ± 0.14	-0.07 ± 0.69	1.61 ± 0.13	6.33 ± 0.61
2	0.20 ± 0.06	2.40 ± 0.28	0.91 ± 0.10	0.93 ± 0.50	0.78 ± 0.07	1.37 ± 0.32	1.21 ± 0.07	5.85 ± 0.33

^a ΔH° values are given in kcal·mol⁻¹.^b ΔS° values in cal kcal mol⁻¹.

Table V. ΔG° Values Calculated by Eq. (1) from Data Presented in Table IV

Compound	T (K) ^a	ΔG° (kcal·mol ⁻¹) ^b			
		CD ₂ Cl ₂	CD ₃ OD	(CD ₃) ₂ CO	C ₇ D ₈
1	183	0.08	0.72	0.54	0.45
	243	-0.07	0.66	0.55	0.07
	298	-0.2	0.61	0.55	-0.28
	183	-0.24	0.74	0.53	0.14
2	243	-0.38	0.68	0.45	-0.21
	298	-0.51	0.63	0.37	-0.53

^aValues relate to the ends of the experimental temperature interval and to room temperature.

^bCalculated deviations are less than 5%.

Kinetic Parameters of the Conformational Exchange I → II

The conformer interconversion of compounds **1** and **2** was also investigated by the complete band-shape analysis over a temperature interval of 233 to 313 K. The I → II system was described as one-spin two-sites nonmutual exchange and 6-H triplets were simulated. In performing these simulations, we assumed that the NMR line widths (in the absence of exchange broadening) and the activation energies have negligible temperature dependence. A temperature-independent line width corresponding to an effective relaxation time $T_2^* = 0.1$ s was assumed for each type of proton. Our simulations did not account for differences in the relevant signal shapes between the conformers due to several, weak spin-couplings. The chemical shifts and the line widths are extrapolated from the slow-exchange region to the region of faster exchange. While the relative populations of I and II conformers were held fixed at the calculated values, the interconversion rate constants of the I → II process (k_{I-II}) were allowed to vary, until qualitative agreement between simulated and experimental line shape was achieved for each temperature (Fig. 3).

The obtained rate constants clearly show that, with rising a temperature, factors favoring conformer II over I are more pronounced for lactone **2** (Table VI).

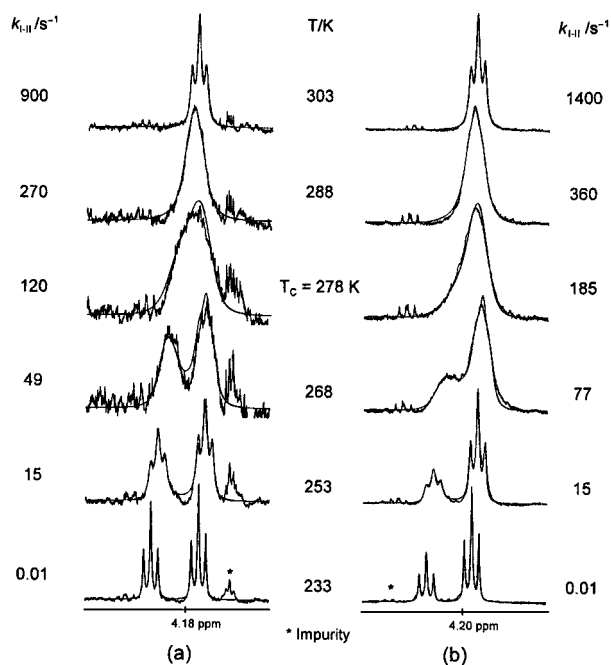


Fig. 3. Experimental (CD₂Cl₂, noisy line) and simulated (smooth line) 6-H triplets of the conformers I and II, at selected temperatures: (a) compound **1**; (b) compound **2**.

The activation energies E_a were calculated from the Arrhenius Eq. (2):

$$k = Ae^{-(E_a/RT)} \quad (2)$$

and its linear form ($\ln k = \ln A - E_a/RT$) allowed for the linear simple least-squares analysis illustrated in Fig. 4.

The obtained E_a values are 12.78 ± 0.35 and 15.11 ± 0.64 kcal·mol⁻¹, for compounds **1** and **2**, respectively.

Geometry Optimization

Resemblance between lactones **1** and **2** was confirmed by the results of their geometry optimization. For

Table VI. Interconversion Rates of I⇌II Processes for Lactones **1** and **2** Gained by ¹H NMR Dynamic Simulation at All Experimental Temperatures

Compound	Reaction	k (s ⁻¹)											
		233 K	243 K	253 K	263 K	268 K	273 K	278 K	283 K	288 K	293 K	303 K	313 K
1	I→II	0.01	4	15	47	49	73	120	200	270	500	900	1600
	II→I ^a	0.01	3.4	11	34	35	53	87	145	195	362	652	1159
2	I→II	0.01	2	15	55	77	120	185	300	360	570	1400	4100
	II→I ^a	0.01	0.8	6.44	24	33	51	79	129	154	244	600	1757

^a $k_{II-I} = k_{I-II} [I]/[II]$; [I] and [II] are the populations of conformers I and II, respectively, estimated on the integral values of 6-H NMR signals.

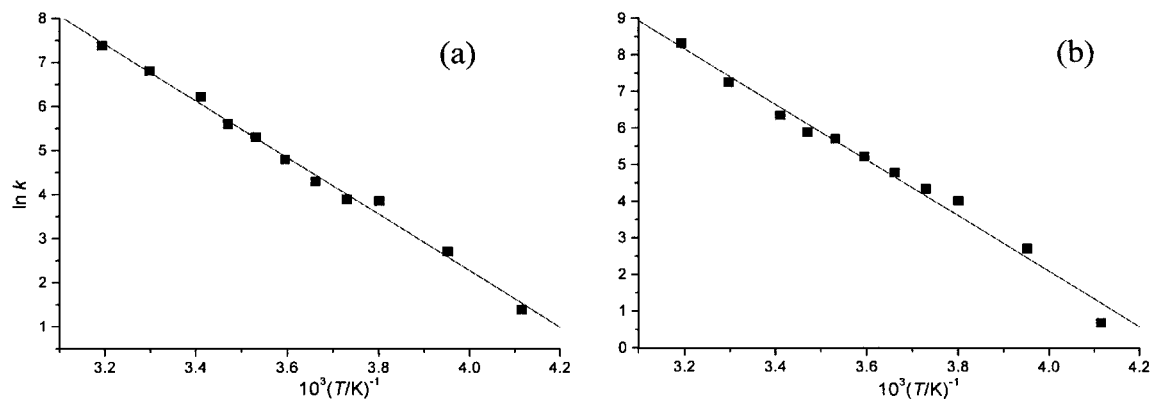


Fig. 4. Linear plot of the rate constants for I→II process versus temperature according to Eq. (2): (a) compound **1**, $r = -0.997$; (b) compound **2**, $r = -0.992$.

both, **1** and **2**, semiempirical PM3 calculations predicted four distinctive conformations that we assigned: I, Ia, II, and III (Fig. 5).

The essential difference between resultant geometries is conformation of the heptane ring. Conformers I and Ia are so similar that NMR spectra would hardly distinguish them: cycloheptane is a chair in I and slightly

distorted chair in Ia (in both, I and Ia, OR₁ and OH are pseudo-equatorial, while OR₂ and 10-CH₃ are pseudo-axial). Heptane ring adopts twisted chair geometry in conformer II, i.e., bulky OR₂ and 10-CH₃ are pseudo-equatorial and OR₁ is in a position where both orientations (eq./ax.) are isoenergetic (C-8 atom of lactones **1–5** corresponds to C-1 atom of unsubstituted heptane ring) [5]. In

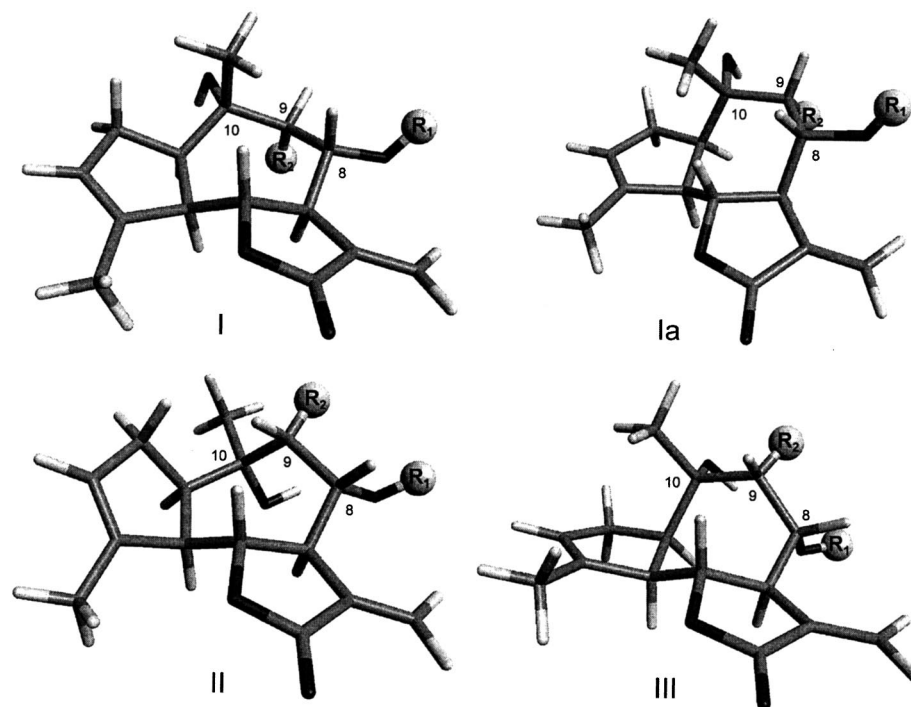


Fig. 5. Low energy conformations of guaianolides **1** ($R_1 = \text{Ac}$, $R_2 = \text{OAc}$) and **2** ($R_1 = i\text{-But}$, $R_2 = \text{OAc}$) found by the PM3 semiempirical calculations.

conformer III, cycloheptane has distorted boat geometry (Fig. 5).

Analyzing low-temperature 1D (^1H and ^{13}C) NMR spectra and characteristic correlations in 2D NMR spectra (DQF COSY, PS NOESY, HSQC, HMBC) of compounds **1** [2a] and **2** [2b], one could conclude that 10-CH₃ is pseudoaxial in conformer I ($\delta_c = 21.7$ ppm; nOe correlations: 14-H/9-H, 14-H/8-H, and 14-H/6-H for both, **1** and **2**), and pseudoequatorial in conformer II ($\delta_c = 27.9$ ppm for **1**, $\delta_c = 27.6$ ppm for **2**; nOe correlations: 9-H/6-H, 9-H/2-H β , and 1-H/14-H for both, **1** and **2**). Consequently, cycloheptane is in a chair conformation in conformer I and in a twisted chair conformation in conformer II. Characteristic differences between conformers I and II of lactones **1** and **2** are vicinal coupling constants $J_{7,8}$ and $J_{8,9}$ in their ^1H NMR spectra. In an attempt to form a relation between experimentally established and calculated geometries, we applied three versions of the Karplus equation [6] to the corresponding dihedral angles. Equation (3) (i.e., the reparametrized standard Karplus equation [6b]) gave the best concordance with experimental results (Table VII; Φ relates to H-C(7)-C(8)-H and to H-C(8)-C(9)-H for $J_{7,8}$ and $J_{8,9}$, respectively).

$$J = A \cos^2 \Phi + B \cos \Phi + C \quad (A = 7.76, \\ B = -1.0, C = 1.40) \quad (3)$$

Comparing the geometries (Table VII) it is obvious that experimentally deduced conformation I well agrees with theoretically calculated conformation I (or I + Ia) and that experimental conformation II suits calculated conformation II for both **1** and **2**. Data from Table VII confirmed that conformer III should be ignored.

The geometry optimization also revealed that, if 10-OH hydroxyl proton and carbonyl O-atom of an OR-moiety (at C-8 or C-9) are suitably oriented, there are possibilities for intramolecular hydrogen bonding only in

rotamers of conformation II (Fig. 6). Moreover, it should be emphasized that 10-OH is pseudoequatorial in conformer I, and, thus, more available for intermolecular hydrogen bonding with solvent molecules. Consequently, this interaction could be the essential one for, experimentally observed, domination of the conformer I in polar solvents [CD_3OD and $(\text{CD}_3)_2\text{CO}$; Table I]. At higher temperatures, this interaction weakens and the population of energetically less stable conformer II increases. A lack of intermolecular hydrogen bonds allows more expressive ring inversion in nonpolar solvents. Relatively large ΔS° values (Table IV), as well as the possibility of intramolecular hydrogen bonding (Fig. 6) are the factors acting in the same direction—favoring conformer II in nonpolar solvents (CD_2Cl_2 and C_7D_8) more than in polar ones (particularly for **2** in CD_2Cl_2), as the NMR experiments initially revealed (Table I).

Results of the Geometry Optimization of 9 α -Hydroxycumambrine A (**3**), 9 α -Acetoxy-cumambrine B (**4**), and Cumambrine B (**5**) Regarding NMR Data

The inseparable, isomeric guaianolides **3** and **4** (Fig. 1) were isolated as a mixture with ratio $\mathbf{3}/\mathbf{4} = 15/85$ during previous investigations [2c]. In the ^1H NMR spectrum of the mixture (r.t., CDCl_3), compound **3** appears with sharp, well-resolved signals, while signals of lactone **4** are broadened (similar, but less than for compounds **1** and **2**). The ^1H NMR data were assigned by means of DQF COSY, PS NOESY, HSQC, and HMBC spectra of the mixture. The nOe correlations and the other NMR data suggested that lactone **3** adopts conformation I related to lactones **1** and **2** (*vide supra*). Slightly broadened NMR lines of lactone **4**, typical for a conformational exchange of a medium rate (on NMR time scale), indicate that in conformational mixture dominates conformer II, already defined for compounds **1** and **2** (*vide supra*).

Cumambrine B **5** could be described as the least structural factor contained in compounds **1–4** (Fig. 1). According to the reported NMR data [7], lactone **5** adopts a rigid conformation with heptane ring in twisted chair geometry.

Very similar to lactones **1** and **2**, optimization of geometries **3–5** by PM3 semiempirical method resulted in four conformations, I, Ia, II, and III (Fig. 5) and again, regarding calculated and measured relevant coupling constants, conformer III could be disregarded (Tables VIII and IX). Data from Table VIII confirm that lactone **3**, most likely, prefers conformation I (or I + Ia), while conformation of lactone **4** closely relates to calculated geometry II

Table VII. Calculated and Experimental $^3J_{\text{HH}}$ (in Hz) for Conformers of Compounds **1** and **2**

Compound	Conformer	$J_{\text{calc.}}$		$J_{\text{exp.}}^a$	
		$J_{7,8}$	$J_{8,9}$	$J_{7,8}$	$J_{8,9}$
1	I	9.96	2.2		
	Ia	9.19	2.74	11.1	2.6
	II	9.19	3.83	9.1	5.1
	III	4.17	2.3		
2	I	9.98	2.15		
	Ia	9.17	2.61	10.9	2.5
	II	9.45	4.3	8.8	5.0
	III	5.63	2.71		

^a CD_2Cl_2 , $T < 220$ K.

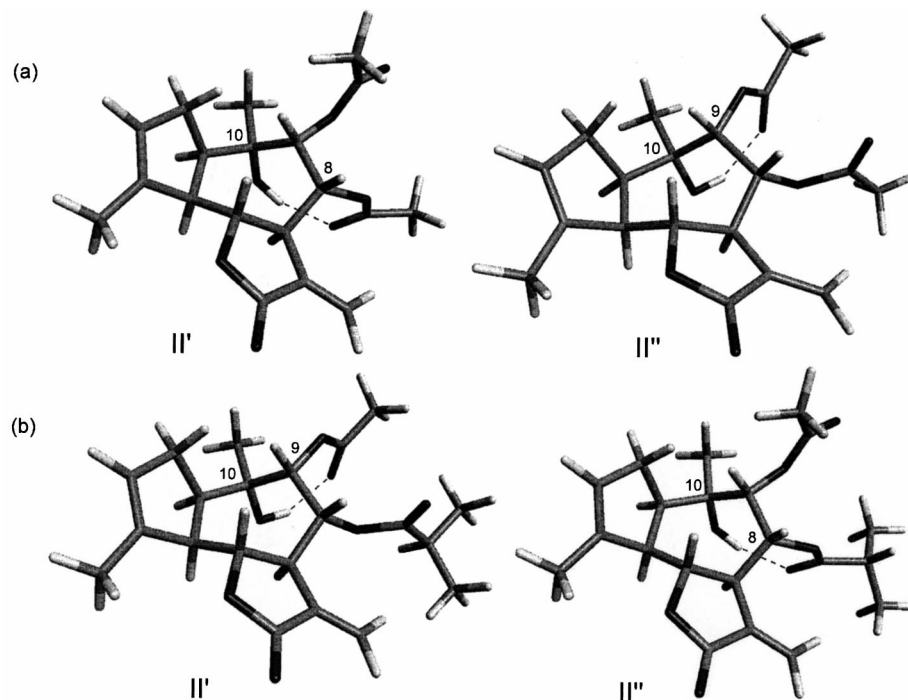


Fig. 6. PM3 calculated rotamers of conformation II with intramolecular hydrogen bonds: (a) compound 1; (b) compound 2.

(Fig. 5, $R_1 = \text{Ac}$, $R_2 = \text{OH}$ and $R_1 = \text{H}$, $R_2 = \text{OAc}$ for **3** and **4**, respectively).

In the case of cumambrine B **5**, comparison of calculated geometries with experimental results is of little help, since experimental coupling constants pretty well agree with those calculated for all three significant conformers (Table IX).

However, calculated geometry II (Fig. 5, $R_1 = R_2 = \text{H}$), with cycloheptane in twisted chair conformation, was

deduced also from the geminal couplings and paramagnetic shift of exomethylene protons [1f, 7a], so it should be the most probable conformation of cumambrine B **5**.

CONCLUSIONS

The results of the conformational analysis obtained by low-temperature NMR experiments, also supported by PM3 semiempirical calculations, indicate that conformational exchange of compounds **1** and **2** occurs between two distinctive conformers, I and II, comprising

Table VIII. Relevant $^3J_{\text{HH}}$ (in Hz) for Lactones **3** and **4**

Compound	Conformer	$J_{\text{calc.}}^a$		$J_{\text{exp.}}^b$	
		$J_{7,8}$	$J_{8,9}$	$J_{7,8}$	$J_{8,9}$
3	I	9.91	1.95	10.9	2.8
	Ia	9.31	2.5		
	II	9.3	4.4		
4	III	4.5	2.6	8.6	4.5
	I	10.1	2.4		
	Ia	9.92	3.1		
	II	9.29	4.23		
	III	5.5	2.5		

^aBy Eq. (3).

^b CDCl_3 , r.t.

Table IX. Relevant $^3J_{\text{HH}}$ (in Hz) for Lactone **5**

Conformer	$J_{\text{calc.}}^a$		
	$J_{5,6}$	$J_{6,7}$	$J_{7,8}$
I	9.72	8.39	10.18
Ia	9.91	7.7	9.73
II	10.25	7.99	9.33
III	10	8.52	5.7
$J_{\text{exp.}}^b$	9.4	10	10

^aBy Eq. (3).

^bRef. [7d].

“chair \rightleftharpoons twisted chair” interconversion of the heptane ring. As ^1H NMR spectra show, the conformational equilibrium virtually depends on the solvent's polarity and, to a lesser degree, on temperature. The thermodynamic parameters of the exchange reaction $\text{I} \rightleftharpoons \text{II}$ and the results of the geometry optimization suggest that the position of conformational equilibrium is attributable to two sets of factors: relative energies and intermolecular interactions favoring conformation I at low temperatures and entropy factor and intramolecular interactions favoring conformer II at higher temperatures. The rate constants and Arrhenius activation energies for the conversion $\text{I} \rightarrow \text{II}$ of lactones **1** and **2** were deduced from dynamic NMR simulations. Relatively high E_a values (~ 13 and 15 kcal mol^{-1} , for **1** and **2**, respectively) if compared with interconversion barriers of unsubstituted cycloheptane [5] are, probably, consequence of unfavorable van der Waals interactions among the substituents in the transition geometries on the pseudorotational coordinate of the $\text{I} \rightarrow \text{II}$ reaction. The E_a is higher for lactone **2**, but not high enough to prevent the exchange process led by positive entropy difference. Slightly different conformational behavior of compounds **1** and **2** apparently originates from the single difference between them—bulky *i*-But-group in lactone **2**, versus Ac-group in **1**.

The calculated geometries of the guaianolides **3–5** are in a very good concordance with experimental (NMR) data, as well.

ACKNOWLEDGMENTS

The authors from Serbia and Montenegro are grateful to the serbian Ministry for Science, Technology and Development for financial support. One of us (NT) thanks

the Mayo Foundation and DAAD for grants and Dr. Eline Basilio-Janke (FU Berlin) for technical assistance in some NMR experiments.

REFERENCES

- (a) McPhail, A. T.; Sim, G. A. *Tetrahedron* **1973**, *29*, 1751; (b) Sosa, V. E.; Oberti, J. C.; Gil, R. R.; Ruveda, E. A.; Goedken, V. L.; Cutierrez, A. B.; Herz, W. *Phytochemistry* **1989**, *28*, 1925; (c) Barrero, A. F.; Sanchez, J. F.; Molina, J.; Barron, A.; del Mar Salas, M. *Phytochemistry* **1990**, *29*, 3575; (d) Spring O.; Zipper, R.; Vogler, B.; Callegari Lopes, J. L.; Vichnewski, W.; Aparecida Dias, D.; Cunha, W. R. *Phytochemistry* **1999**, *52*, 79; (e) Schorr, K.; Garcia-Pineres, A. J.; Siedle, B.; Merfort, I.; Da Costa, F. B. *Phytochemistry* **2002**, *60*, 733; for stereochemistry of some specific fragments, see also: (f) Samek, Z.; Holub, M.; Vokač, K.; Droždž, B.; Jommi, G.; Gariboldi, P.; Corbella, A. *Collect. Czech. Chem. Commun.* **1972**, *37*, 2611; (g) Holub, M.; Samek, Z.; Vašičkova, S.; Masojdkova, M. *Collect. Czech. Chem. Commun.* **1978**, *43*, 2444.
- (a) Milosavljević, S.; Vajs, V.; Bulatović, V.; Đoković, D.; Aljančić, I.; Juranić, N.; Macura, S. *Recent Res Develop Phytochem.* **1998**, *2*, 383; (b) Vajs, V.; Todorović, N.; Bulatović, V.; Menković, N.; Macura, S.; Juranić, N.; Milosavljević, S. *Phytochemistry* **2000**, *54*, 625; (c) Bulatović, V.; Vajs, V.; Macura, S.; Juranić, N.; Milosavljević, S. *J. Nat. Prod.* **1997**, *60*, 1222; (d) Bruno, M.; Maggio, A.; Arnold, N. A.; Diaz, J. G.; Herz, W. *Phytochemistry* **1998**, *49*, 1739.
- Braun, S.; Kalinowski, H.- O.; Berger, S. *100 and More Basic NMR Experiments*; VCH: Weinheim, 1996.
- Binsch, G. J. *J. Amer. Chem. Soc.* **1969**, *91*, 1304.
- (a) Hendrickson, J. B. *J. Amer. Chem. Soc.* **1961**, *83*, 4537; (b) Hendrickson, J. B. *Tetrahedron* **1963**, *19*, 1387; (c) Engler, E. M.; Andose, J. D.; von R. Schleyer, P. *J. Amer. Chem. Soc.* **1973**, *95*, 8005; (d) Kolossváry I.; Guida, W. C. *J. Amer. Chem. Soc.* **1993**, *115*, 3107; (e) Eliel, E. L.; Allinger, N. L.; Angyal, S. J.; Morrison, G. A. *Conformational Analysis*; Wiley: New York, 1966.
- (a) Karplus, M. *J. Amer. Chem. Soc.* **1963**, *85*, 2870; (b) Haasnoot, C. A. G.; Leeuw, F. A. A. M.; Altona, C. *Tetrahedron* **1980**, *36*, 2783 [Eqs. (5) and (8)].
- (a) Romo, J.; Romo de Vivar, A.; Diaz, E. *Tetrahedron* **1968**, *24*, 5625; (b) Yoshioka, H.; Mabry, T. J.; Irwin, M. A.; Geissman, T. A.; Samek, Z. *Tetrahedron* **1971**, *27*, 3317; (c) Yoshioka, H.; Mabry, T. J.; Timmermann, B. N. *Sesquiterpene Lactones-Chemistry, NMR and Plant Distribution*; University of Tokyo Press: Japan, 1973; (d) Bulatović, V. M. PhD thesis, Belgrade, 1998.